

Power scale-up of high-pulse-energy passively Q-switched Nd:YLF laser: influence of negative thermal lens enhanced by upconversion

This content has been downloaded from IOPscience. Please scroll down to see the full text.

2012 Laser Phys. Lett. 9 625

(<http://iopscience.iop.org/1612-202X/9/9/001>)

View [the table of contents for this issue](#), or go to the [journal homepage](#) for more

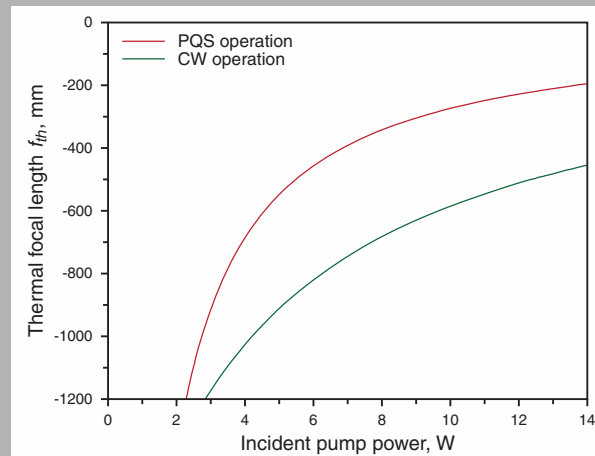
Download details:

IP Address: 140.113.38.11

This content was downloaded on 28/04/2014 at 22:09

Please note that [terms and conditions apply](#).

Abstract: We develop a practical method to extend the power scale-up for a laser in a concave-plano cavity to be influenced by a large negative thermal lens. With the developed method, we successfully scale up the output power of a compact high-pulse-energy passively Q-switched Nd:YLF laser at 1053 nm with the Cr^{4+} :YAG crystal as a saturable absorber. At an incident pump power of 12.6 W, the maximum output power under the optimum operation at 1053 nm reaches 2.61 W with a pulse width of 6 ns and a pulse repetition rate of 4.6 kHz. More importantly, we experimentally verify that the energy-transfer upconversion significantly enhances the negative focal length of thermal lens in the passively Q-switched Nd:YLF laser.



Numerical calculations of the thermal focal length *versus* the incident pump power for the CW and PQS cases

© 2012 by Astro, Ltd.

Power scale-up of high-pulse-energy passively Q-switched Nd:YLF laser: influence of negative thermal lens enhanced by upconversion

Y.J. Huang, C.Y. Tang, Y.P. Huang, S.C. Huang, K.W. Su, and Y.F. Chen*

Department of Electrophysics, National Chiao Tung University, Hsinchu, Taiwan

Received: 13 February 2012, Revised: 25 February 2012, Accepted: 1 March 2012

Published online: 12 June 2012

Key words: passive Q-switching; thermal lens; energy-transfer upconversion; Nd:YLF

1. Introduction

Diode-pumped solid-state lasers are useful in a great number of industrial applications and scientific researches. Passive Q-switching of the solid-state laser with a saturable absorber provides a reliable pulsed operation that takes the advantages of high stability, inherent compactness, and low cost [1–3]. The laser crystal with long fluorescence lifetime is highly desirable for continuously pumped passively Q-switched (PQS) laser to generate high-energy pulses. Consequently, the Nd:YLF crystal that is characterized by relatively long upper-state lifetime has large potential for developing a high-pulse-energy pulsed

laser with the Cr^{4+} :YAG saturable absorber. Moreover, the Nd:YLF laser is inherently beneficial to be a master oscillator for the Nd:Glass power amplifier due to the excellent spectral overlap between the 1053-nm emission line and the gain peak of the Nd:Glass laser [4].

Practically, using the c-cut Nd:YLF crystal is a convenient way for generating the emission line at 1053 nm, because it can completely avoid the complexities required for the suppression of the unwanted laser transition at 1047 nm. The fluorescence lifetime of 540 μs at 1053 nm in the c-cut Nd:YLF crystal is also expected to be more suitable for producing high-energy pulses as compared with that of 490 μs at 1047 nm in the a-cut counterpart [3].

* Corresponding author: e-mail: yfchen@cc.nctu.edu.tw

However, the implementation of high-pulse-energy PQS Nd:YLF lasers at 1053 nm has not been completely explored yet. The main reason is that the behavior of the thermal-lensing effect in the c-cut Nd:YLF crystal is significantly different from the ones in other popular gain media such as Nd:YVO₄ and Nd:YAG crystals. The critical difference is that the negative dependence of the refractive index on the temperature (dn/dT) over the positive contribution from the end-face bulging of the gain medium leads the c-cut Nd:YLF crystal to behave a defocusing thermal lens. Furthermore, the effect of the energy-transfer upconversion (ETU) reduces the effective upper-state lifetime and increases the fractional thermal loading in the laser crystal [5–8]. The ETU effect inevitably causes the effective focal length of the thermal lens in the PQS operation to be considerably more negative than the one in the continuous wave (CW) operation. As a result, a reliable and efficient tactic for designing continuously pumped high-pulse-energy PQS laser at 1053 nm is highly desirable to be developed.

In this work, we develop a straightforward method to implement the power scale-up of a compact high-pulse-energy PQS Nd:YLF laser at 1053 nm with the Cr⁴⁺:YAG crystal as a saturable absorber in a concave-plano cavity. We numerically analyze the mode-to-pump size ratio as a function of the thermal focal length to verify that decreasing the radius of curvature (ROC) of the concave mirror can effectually extend the power scale-up for a laser in a concave-plano cavity to be influenced by a large negative thermal lens. With the developed method, we experimentally make a systematic comparison between the CW and PQS operations of the c-cut Nd:YLF laser to confirm the negative thermal-lensing effect enhanced by the ETU effect. At an incident pump power of 12.6 W, the optimum 1053-nm laser produces the maximum output power of 2.61 W with a pulse width of 6 ns and a pulse repetition rate of 4.6 kHz. The corresponding pulse energy and peak power are estimated to be up to 570 μ J and 95 kW, respectively. To the best of our knowledge, these are the largest pulse energy and highest peak power ever reported among continuously pumped PQS Nd-doped crystal/Cr⁴⁺:YAG lasers with the same initial transmission.

2. Numerical analyses

Previous studies have demonstrated that the mode-to-pump size ratio plays an important role for power scaling in diode-end-pumped solid-state lasers, in which the optimum mode-to-pump size ratio is practically found to be in the range 0.6–1.0 [9–11]. With the ABCD-matrix theory, here we take into account of the thermal-lensing effect to numerically calculate the mode-to-pump size ratio as a function of the thermal focal length for the cases of $R = 50$ mm, 100 mm, 200 mm, and 500 mm in a concave-plano cavity, where R is the ROC of the input concave mirror. In the present analyses, the pump radius $\omega_{p0} = 210$ μ m

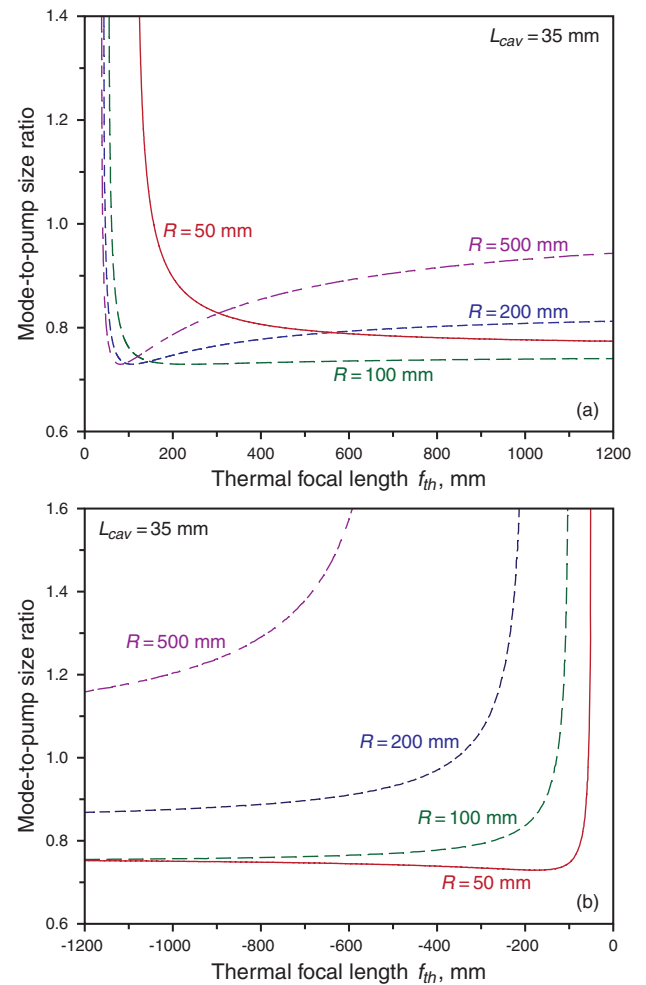


Figure 1 (online color at www.lasphys.com) Calculated results for the mode-to-pump size ratio as a function of the thermal focal length for the cases of $R = 50$ mm, 100 mm, 200 mm, and 500 mm. (a) – positive thermal-lensing effect and (b) – negative thermal-lensing effect

and the cavity length $L_{cav} = 35$ mm are used, and the thermally induced lens is set to be adjacent to the input concave mirror.

When the positive thermal lens is considered, we find that the mode-to-pump size ratios for all cases are well located between 0.6–1.0 in the large operated region, as depicted in Fig. 1a. We also find that the magnitude of the thermal focal length $|f_{th}|$ should be larger than $(RL)/(R-L)$ to satisfy the stability criterion. Because the magnitude of the thermal focal length is inversely proportional to the incident pump power, the higher incident pump power can be allowed by using the concave mirror with larger ROC when the positive thermal lens is regarded.

On the other hand, we find that the ROC of the concave mirror needs to be small enough to fulfill the optimum mode-to-pump size ratio for the case of negative thermal-

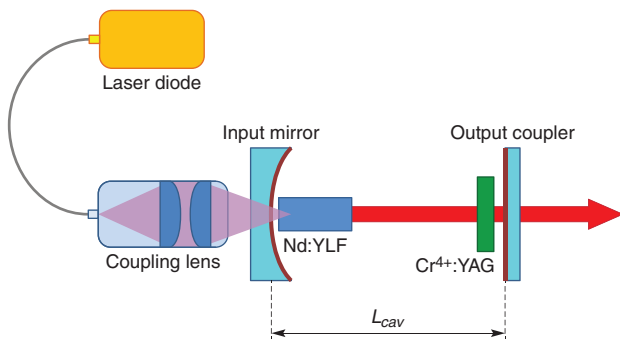


Figure 2 (online color at www.lasphys.com) Configuration of the cavity setup for a diode-pumped PQS Nd:YLF/Cr⁴⁺:YAG laser

lensing effect, as shown in Fig. 1b. At the same time, the magnitude of the thermal focal length $|f_{th}|$ is derived to need to be larger than R to keep the cavity stable. On the whole, it is numerically found that decreasing the ROC of the concave mirror is favorable for simultaneously achieving good mode-to-pump size ratio as well as power scaling in a concave-plano cavity that is affected by a negative thermal lens.

3. Experimental setup

The experimental setup is schematically shown in Fig. 2. The input concave mirror was antireflection (AR) coated at 806 nm on the entrance face, and was coated for high transmission at 806 nm as well as for high reflection at 1053 nm on the second surface. The gain medium was a 0.8 at.% c-cut Nd:YLF crystal with the diameter of 4 mm and the length of 15 mm. The Nd:YLF crystal was placed adjacent to the input concave mirror. Both facets of the laser crystal were AR coated at 806 and 1053 nm. The Cr⁴⁺:YAG saturable absorber with an initial transmission of 80% was AR coated at 1053 nm on both surfaces, and it was placed near to the output coupler for achieving a high-quality PQS operation. The laser crystal and the saturable absorber were wrapped with indium foil and mounted in water-cooled copper heat sinks at 16°C. The pump source was a fiber-coupled laser diode at 806 nm with a core diameter of 400 μm and a numerical aperture of 0.14. The pump beam with the spot radius of 210 μm was re-imaged inside the laser crystal with a lens set that has the focal length of 25 mm and the coupling efficiency of 90%. The flat output coupler with the reflectivity of 74% at 1053 nm was employed throughout the experiment. The cavity length was set to be 35 mm for the construction of a compact PQS laser. The pulse temporal behaviors were recorded by a LeCroy digital oscilloscope (Wavepro 7100, 10 G samples/s, 1 GHz bandwidth) with a fast InGaAs photodiode.

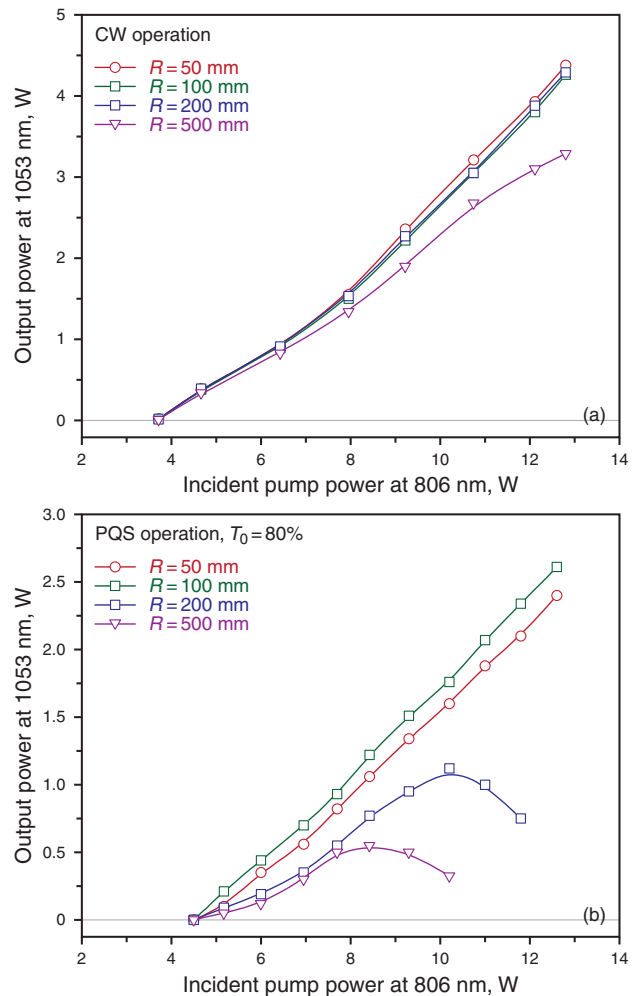


Figure 3 (online color at www.lasphys.com) Output power as a function of the incident pump power for the cases of $R = 50$ mm, 100 mm, 200 mm, and 500 mm. (a) – in the CW operation and (b) – in the PQS operation

4. Performance of CW and PQS operations

First of all, the CW operation without the saturable absorber was studied. Fig. 3a shows the output power at 1053 nm as a function of the incident pump power at 806 nm for the cases of $R = 50$ mm, 100 mm, 200 mm, and 500 mm. It is obvious that although the pump thresholds for all cases are almost identical, the slope efficiency obtained with $R = 500$ mm is remarkably lower than those obtained with other three cases. This observation is a result of the poorer mode-to-pump size ratio, as can be referred to Fig. 1b for $R = 500$ mm case.

When the Cr⁴⁺:YAG saturable absorber was inserted into the resonator, the degradation in the output power together with the roll-over phenomena for $R = 200$ mm and 500 mm in the PQS operation further highlight the crucial importance of using small ROC of the concave mirror for

power scale-up, as depicted in Fig. 3b. During the early researches on the Nd:YLF crystal, many investigations indicated that power scaling in the Nd:YLF laser is practically hindered by the ETU effect [5–8]. The combined effect of the ETU effect and its subsequent multiphonon relaxation brings in the considerable enhancement of the thermal-lensing effect in the Nd:YLF laser. As a consequence, the increased thermal-lensing effect in the present PQS operation is believed to cause the deterioration in the output powers for $R=200$ mm and 500 mm. From the analyses of the coupled rate equation, the criterion for good PQS operation is given by [12]:

$$\frac{\ln\left(\frac{1}{T_0^2}\right)}{\ln\left(\frac{1}{T_0^2}\right) + \ln\left(\frac{1}{R_{OC}}\right)} \frac{\sigma_{gs}}{\sigma} \frac{A}{A_s} \gg \frac{\gamma}{1-\beta}, \quad (1)$$

where T_0 is the initial transmission of the saturable absorber, R_{OC} is the reflectivity of the output coupler, L is the nonsaturable loss, σ_{gs} is the ground-state absorption cross section of the saturable absorber, σ is the stimulated emission cross section of the gain medium, A/A_s is the ratio of the mode area in the gain medium and in the saturable absorber, γ is the inversion reduction factor, and β is the ratio of the excited-state absorption cross section to the ground-state absorption cross section in the saturable absorber. Since the σ_{gs} value of the Cr⁴⁺:YAG crystal ($\sim(20\pm 5)\times 10^{-19}$ cm²) is remarkably larger than the σ value of the Nd:YLF crystal (1.2×10^{-19} cm²), the criterion for good PQS operation is generally satisfied in the Nd:YLF/Cr⁴⁺:YAG laser despite the ratio of the mode area A/A_s varies with the incident pump power and the ROC of the concave mirror. In other words, the influence of the changing mode area in the saturable absorber on the PQS performance can be neglected undoubtedly.

To further investigate the influence of the negative thermal lens on the Nd:YLF laser, we evaluate the effective focal length of the thermal lens with the following equation [13,14]:

$$\frac{1}{f_{th}} = \quad (2)$$

$$= \frac{\xi P_{in}}{\pi K_c} \int_0^l \frac{\alpha e^{-\alpha z}}{1 - e^{-\alpha z}} \frac{1}{\omega_p^2(z)} \left[\frac{1}{2} \frac{dn}{dt} + (n-1)\alpha_T \frac{\omega_P(z)}{l} \right] dz,$$

$$\omega_p(z) = \omega_{p0} \sqrt{1 + \left[\frac{M^2 \lambda_p}{n\pi \omega_{p0}^2} (z - z_0) \right]^2}, \quad (3)$$

where ξ is the fractional thermal loading, P_{in} is the incident pump power, K_c is the thermal conductivity of the laser crystal, l is the length of the laser crystal, α is the absorption coefficient at the pump wavelength λ_p , dn/dT is the temperature dependence of the refractive index, n is the refractive index, α_T is the coefficient of the thermal expansion, M^2 is the pump beam quality factor, and



Figure 4 (online color at www.lasphys.com) Numerical calculations of the thermal focal length *versus* the incident pump power for the CW and PQS cases

$\omega_p(z)$ is the variation of the pump radius, where the pump beam waist ω_{p0} is assumed a distance z_0 from the entrance of the laser crystal. With the following parameters: $K_c = 6.3$ W/m K, $l = 15$ mm, $\alpha = 0.18$ mm⁻¹, $\lambda_p = 806$ nm, $dn/dT = -2\times 10^{-6}$ K⁻¹, $n = 1.448$, $\alpha_T = 8.3\times 10^{-6}$ K⁻¹, $M^2 = 115$, $\omega_{p0} = 210$ μ m, and $z_0 = 3.8$ mm, the thermal focal length with respect to the incident pump power is plotted in Fig. 4. Numerical calculations for the CW case with $\xi = 0.24$ are found to be consistent with the previously published data, where the fractional thermal loading ξ is derived from the quantum defect value. According to the previous studies, the fractional thermal loading influenced by the ETU effect is usually magnified by a factor of ~ 3 as compared with the value in the CW operation. Therefore, we use $\xi = 0.7$ to calculate the PQS case, as revealed in Fig. 4. Numerical calculations for the PQS case are found to be in good agreement with the estimated results deduced from the experimental data shown in Fig. 3b. The deduction is based on the fact that the ROC of the concave mirror needs to be smaller than the magnitude of the thermal focal length to satisfy the stability criterion, as analyzed in Sec. 2. To be brief, a concave mirror with the ROC significantly smaller than the thermal focal length can be effectively used to achieve the power scale-up for a laser influenced by a negative thermal lens with a plano-concave cavity. Moreover, due to the ETU effect, the suitable ROC of the concave mirror for the PQS case is considerably smaller than that for the CW case at the same incident pump power.

In Fig. 3b, the resonator with $R = 100$ mm is found to possess the highest maximum output power of 2.61 W at an incident pump power of 12.6 W. Therefore, we make a thorough study on the performance of the PQS Nd:YLF/Cr⁴⁺:YAG laser with $R = 100$ mm. Fig. 5a and Fig. 5b illustrate the dependences of the pulse width, pulse

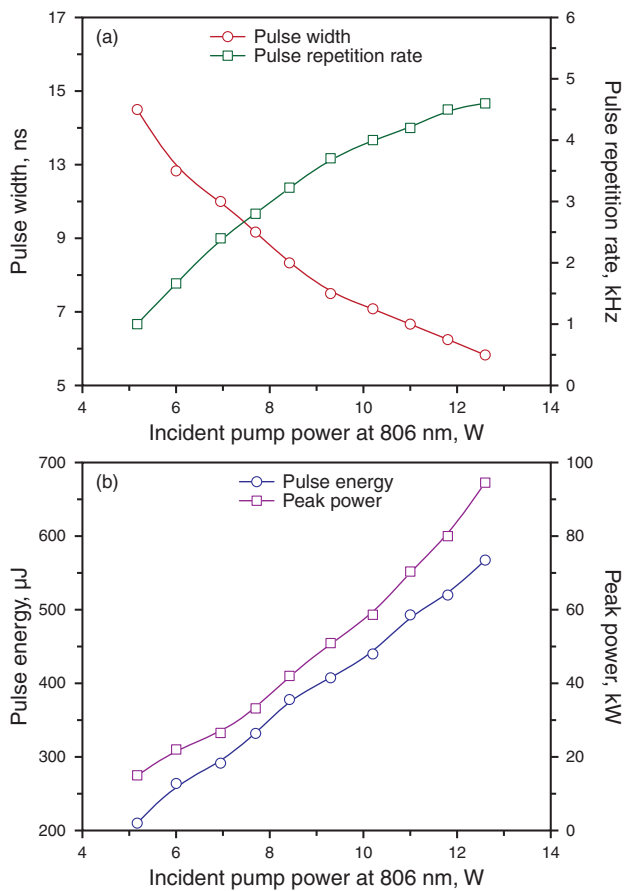


Figure 5 (online color at www.lasphys.com) Dependences of (a) the pulse width, pulse repetition rate and (b) pulse energy, peak power on the incident pump power in the PQS operation with $R = 100$ mm

repetition rate, pulse energy and peak power on the incident pump power. When the incident pump power increases from 5.17 to 12.6 W, the pulse width decreases from 14 ns to 6 ns and the pulse repetition rate varies from 1.0 to 4.6 kHz, as shown in Fig. 5a. Accordingly, it can be seen that the pulse energy increases from 210 to 570 μJ and the peak power changes from 15 to 95 kW with increasing the incident pump power from 5.17 to 12.6 W, as revealed in Fig. 5b. Typical temporal behaviors of the output pulses at an incident pump power of 12.6 W are shown in Fig. 6a and Fig. 6b with the time span of 2 ms and 100 ns, respectively. The pulse-to-pulse amplitude fluctuation is generally found to be within $\pm 3\%$.

Finally, it is worthwhile to mention that so far the pulse energies obtained with the continuously pumped PQS Nd-doped crystal/ Cr^{4+} :YAG lasers, such as the Nd:YAG [1,2], c-cut Nd:YLF [3], Nd-doped vanadate crystals [1], and so on, are not more than ~ 300 μJ . That is to say, the pulse energy based on the ${}^4\text{F}_{3/2} \rightarrow {}^4\text{I}_{11/2}$ transition is significantly enhanced in our present work. This indicates that

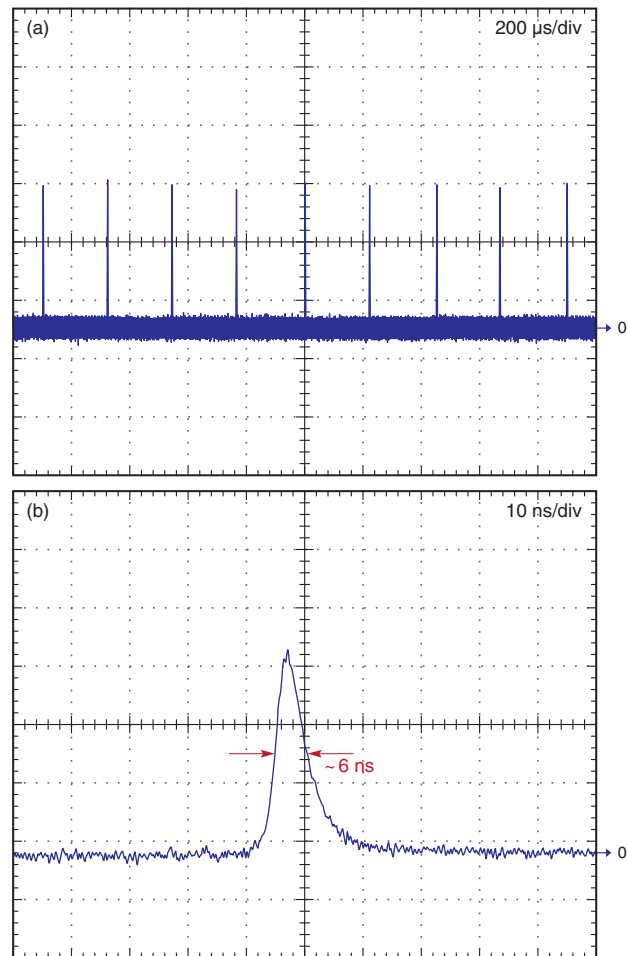


Figure 6 (online color at www.lasphys.com) Typical temporal behaviors at 1053 nm with (a) – time span of 2 ms and (b) – time span of 100 ns

the c-cut Nd:YLF crystal is potentially favorable for the construction of high-pulse-energy lasers as long as the optical resonator is intricately designed to compensate for the large negative thermal-lensing effect in the gain medium.

5. Conclusion

In summary, we have found that decreasing the ROC of the concave mirror can usefully extend the power scale-up for a laser in a concave-plano cavity to be influenced by a large negative thermal lens. With this finding, we have developed a practical tactic to scale up the output power of a compact high-pulse-energy PQS Nd:YLF laser at 1053 nm with the Cr^{4+} :YAG crystal as a saturable absorber. At an incident pump power of 12.6 W, the optimum PQS laser at 1053 nm emits the maximum output power of 2.61 W with a pulse width of 6 ns and a pulse repetition rate of 4.6 kHz. The corresponding pulse energy and peak power are up to

570 μJ and 95 kW, respectively. We further experimentally confirmed that the negative focal length of the thermal lens is considerably enhanced by the ETU effect in the PQS Nd:YLF laser.

Acknowledgements The authors thank the National Science Council for their financial support of this research under Contract No. NSC-100-2628-M-009-001-MY3.

References

- [1] A. Agnesi, S. Dell'Acqua, C. Morello, G. Piccinno, G.C. Reali, and Z.Y. Sun, *IEEE J. Sel. Top. Quantum Electron.* **3**, 45–52 (1997).
- [2] N. Pavel, J. Saikawa, S. Kurimura, and T. Taira, *Jpn. J. Appl. Phys.* **40**, 1253–1259 (2001).
- [3] S.D. Pan, K.Z. Han, H.M. Wang, X.W. Fan, and J.L. He, *Chin. Opt. Lett.* **4**, 407–409 (2006).
- [4] A.V. Okishev and W. Seka, *IEEE J. Sel. Top. Quantum Electron.* **3**, 59–63 (1997).
- [5] M. Pollnau, P.J. Hardman, M.A. Kern, W.A. Clarkson, and D.C. Hanna, *Phys. Rev. B* **58**, 16076–16092 (1998).
- [6] P.J. Hardman, W.A. Clarkson, G.J. Friel, M. Pollnau, and D.C. Hanna, *IEEE J. Quantum Electron.* **35**, 647–655 (1999).
- [7] J.D. Zuegel and W. Seka, *Appl. Opt.* **38**, 2714–2723 (1999).
- [8] L.C. Courrol, E.P. Maldonado, L. Gomes, N.D. Vieira, Jr., I.M. Ranieri, and S.P. Morato, *Opt. Mater.* **14**, 81–90 (2000).
- [9] Y.F. Chen, T.M. Huang, C.F. Kao, C.L. Wang, and S.C. Wang, *IEEE J. Quantum Electron.* **33**, 1424–1429 (1997).
- [10] Y.F. Chen, T.M. Huang, C.C. Liao, Y.P. Lan, and S.C. Wang, *IEEE Photon. Technol. Lett.* **11**, 1241–1243 (1999).
- [11] Y.F. Chen, Y.C. Chen, S.W. Chen, and Y.P. Lan, *Opt. Commun.* **234**, 337–342 (2004).
- [12] Y.F. Chen, Y.P. Lan, and H.L. Chang, *IEEE J. Quantum Electron.* **37**, 462–468 (2001).
- [13] W. Koechner, *Solid-State Laser Engineering*, 6th ed. (Springer, Berlin, 2005), chapter 7.
- [14] Y.J. Huang, P.Y. Chiang, H.C. Liang, K.W. Su, and Y.F. Chen, *Opt. Commun.* **285**, 59–63 (2012).